Dicarbonylrhodium(I) complexes of pyridine alcohol ligands and their catalytic carbonylation reaction

A B S T R A C T

Reaction of dimeric complex $[Rh(CO)_2Cl]_2$ with two molar equivalent of pyridine alcohol ligands (L) like 2-hydroxymethylpyridine (**a**), 3-hydroxymethylpyridine (**b**) and 4-hydroxymethylpyridine (**c**) afford the rhodium(I) dicarbonyl complexes $[Rh(CO)_2ClL]$(**1a–c**). The ligands are coordinated to the metal center through N-donor site. The complexes **1** undergo oxidative addition (**OA**) reactions with various alkyl halides (RI) like CH_3I, C_2H_5I to produce Rh(III) complexes of the type $[Rh(CO)(COR)IClL]$, where R = $-CH_3$(**2**), $-C_2H_5$(**3**). Kinetic data for the reaction of **1** with CH_3I indicate a first order reaction. The catalytic activity of the complexes **1** in the carbonylation of methanol was higher than that of the well known species $[Rh(CO)_2I_2]^-$.

© 2008 Elsevier B.V. All rights reserved.

1. Introduction

The rhodium-catalyzed carbonylation of methanol to ethanoic acid is a process of great industrial importance [1–3]. The original $[Rh(CO)_2I_2]^-$ catalyst developed at the Monsanto's laboratories [4] and studied in detail by Foster and Singleton [5,6] is largely used for the industrial production of acetic acid and acetic anhydride. The harsh condition of the commercial process have driven the researchers to synthesize new rhodium complexes bearing electron donating ligands [7], which might facilitate more efficiently the oxidative addition (**OA**) of methyl iodide, a key step in the catalytic cycle [8,9] and, consequently, increases the overall production of acetic acid. Heterocyclic alcohols and aldehydes are of great importance because of their two different types of donor atoms, i.e. N and O, which may form interesting metal complexes. Several transition metal complexes containing heterocyclic alcohols like bidentate 2-hydroxymethylpyridine or 2-hydroxyethylpyridine and tridentate 2,6-di(hydroxymethyl)pyridine have been reported, which may exhibit catalytic activity or as model compounds for different enzymes [10–12]. Rh(I) complexes of heterocyclic aldehydes are active catalyst for carbonylation and transfer hydrogenation reactions [13,14]. As a part of our continuing work [14–21], i.e. the effect of different types of ligands on rhodium-catalyzed carbonylation of alcohol we report here the synthesis of rhodium(I) complexes con-

taining 2-hydroxymethylpyridine, 3-hydroxymethylpyridine and 4-hydroxymethylpyridine ligands and their oxidative reactivity towards different electrophiles like CH_3I, C_2H_5I. The kinetic study of the **OA** reactions of the complexes with CH_3I and the catalytic activity of the complexes on the carbonylation of methanol are also evaluated.

2. Experimental

All the solvents used were distilled under N_2 prior to use. Elemental analyses were done on a Perkin Elmer 2400 elemental analyzer. IR spectra (4000–400 cm^{-1}) were recorded in KBr discs and $CHCl_3$ solution on a Perkin Elmer system 2000 FTIR spectrophotometer. NMR (^1H and ^{13}C) spectra were recorded in $CDCl_3$ solution on a Bruker DPX-300 MHz spectrometer and chemical shift were quoted relative to $SiMe_4$ as an internal standard. The carbonylation of methanol was carried out in a 100 ml mini pressure reactor (Autoclave Engineers, USA) fitted with a pressure gauge and the reaction products were analyzed by GC (Chemito 8510, FID). $RhCl_3 \cdot 3H_2O$ was purchased from M/S Arrora Matthey Ltd., Kolkata. All the ligands were purchased from Aldrich, USA and used as received.

2.1. Starting materials

$[Rh(CO)_2Cl]_2$ was prepared by passing CO gas over $RhCl_3 \cdot 3H_2O$ at 100 °C in presence of moisture [22].

* Corresponding author. Tel.: +91 376 2370081; fax: +91 376 2370011.
  E-mail address: dipakkrdutta@yahoo.com (D.K. Dutta).

2.2. Synthesis of the complexes [Rh(CO)₂ClL](**1**), L = 2-hydroxymethylpyridine (**a**), 3-hydroxymethylpyridine (**b**) and 4-hydroxymethylpyridine (**c**)

[Rh(CO)₂Cl]₂ (100 mg) was dissolved in dichloromethane (10 cm³) and to this solution, a stoichiometric quantity (Rh:L = 1:2) of the respective ligands were added. The reaction mixture was stirred at room temperature (r.t.) for about 30 min and the solvent was evaporated under vacuum. The yellow coloured compounds so obtained were washed with diethyl ether and stored over silica gel in a desiccator.

Analytical data for the complexes **1a**–**c**:

1a: Yield: 93%; Anal. found (calcd.) for C₈H₇ClNO₃Rh(%): C, 31.54 (31.66); H, 2.41 (2.31); N, 4.58 (4.62); selected IR data: 2086, 2010 [ν(CO) cm⁻¹], 1609 [δ(OH) cm⁻¹], ¹H NMR data (δ in ppm): δ 8.66 (H-1, d), δ 8.66–8.61(H-2, m), δ 7.96–7.87 (H-3, m), δ 7.85–7.74 (H-4, m) δ 5.16 (CH₂OH, s), ¹³C NMR data (δ in ppm): δ 160 (C-2), δ 124 (C-3), δ 138 (C-4), δ 69 (CH₂OH), δ 183 (CO).

1b: Yield: 90%; Anal. found (calcd.) for C₈H₇ClNO₃Rh(%): C, 31.55 (31.66); H, 2.27 (2.31); N, 4.56 (4.62); selected IR data: 2078, 2002 [ν(CO) cm⁻¹], 1609 [δ(OH) cm⁻¹], ¹H NMR data (δ in ppm): δ 9.24 (H-1, d), δ 8.97–8.86 (H-2, m), δ 7.44–7.38 (H-3, m), δ 8.47–8.13 (H-4, m), δ 4.70 (CH₂OH, s), ¹³C NMR data (δ in ppm): δ 155 (C-2), δ 133 (C-3), δ 137 (C-4), δ 68 (CH₂OH), δ 185 (CO).

1c: Yield: 91%; Anal. found (calcd.) for C₈H₇ClNO₃Rh(%): C, 31.49 (31.66); H, 2.28 (2.31); N, 4.60 (4.62); selected IR data: 2087, 2018 [ν(CO) cm⁻¹], 1619 [δ(OH) cm⁻¹], ¹H NMR data (δ in ppm): δ 9.19 (H-1, d), δ 7.96 (H-2, d), δ 4.73 (CH₂OH, s), ¹³C NMR data (δ in ppm): δ 156 (C-2), δ 125 (C-3), δ 147 (C-4), δ 68 (CH₂OH), δ 184 (CO).

2.3. Synthesis of [Rh(CO)(COR)ClIL][R = CH₃(**2**); R = C₂H₅(**3**)]

[Rh(CO)₂ClL] (100 mg) was dissolved in dichloromethane (15 cm³) and each of RI (6 cm³) (RI = CH₃I, C₂H₅I,) was added to it. The reaction mixture was then stirred at r.t. for about 7 h and 16 h for CH₃I and C₂H₅I, respectively. The colour of the solution changed from yellow to reddish-brown and the solvent was evaporated under vacuum. The compounds so obtained were washed with diethyl ether and stored over silica gel in a desiccator.

Analytical data for the complexes **2a**–**c**, and **3a**–**c**:

2a: Yield: 88%; Anal. found (calcd.) for C₉H₁₀ClINO₃Rh(%): C, 24.30 (24.27); H, 2.18 (2.25); N, 3.18 (3.15); selected IR data: 2070 [ν(CO) cm⁻¹], 1727 [ν(CO)_acyl cm⁻¹], ¹H NMR data (δ in ppm): δ 9.46 (H-1, d), δ 8.55–8.38 (H-2, m), δ 7.72–7.69 (H-3, m), δ 7.87–7.83 (H-4, m), δ 3.21 (CH₃, s), δ 5.10 (CH₂OH, s), ¹³C NMR data (δ in ppm): δ 160 (C-2), δ 125 (C-3), δ 138 (C-4), δ 70 (CH₂OH), δ 185 (CO), δ 206 [(CO)acyl], δ 49 (CH₃).

2b: Yield: 89%; Anal. found (calcd.) for C₉H₁₀ClINO₃Rh(%): C, 24.31 (24.27); H, 2.15 (2.25); N, 3.11 (3.15); selected IR data: 2075 [ν(CO) cm⁻¹], 1736 [ν(CO)_acyl cm⁻¹], ¹H NMR data (δ in ppm): δ 9.21 (H-1, d), δ 9.48–8.82 m (H-2, m), δ 7.63–7.24 (H-3, m), δ 8.57–8.38 (H-4, m), δ 3.38 (CH₃, s), δ 4.64 (CH₂OH, s), ¹³C NMR data (δ in ppm): δ 154 (C-2), δ 133 (C-3), δ 138 (C-4), δ 151 (C-6), δ 69 (CH₂OH), δ 185 (CO), δ 205 [(CO)acyl], δ 51 (CH₃).

2c: Yield: 87%; Anal. found (calcd.) for C₉H₁₀ClINO₃Rh(%): C, 24.21 (24.27); H, 2.18 (2.25); N, 3.25 (3.15); selected IR data: 2082 [ν(CO) cm⁻¹], 1733 [ν(CO)_acyl cm⁻¹], ¹H NMR data (δ in ppm): δ 9.17 (H-1, d), δ 7.72 (H-2, d), 2.96 (CH₃, s), δ 4.70 (CH₂OH, s), ¹³C NMR data (δ in ppm): δ 157 (C-2), δ 124 (C-3), δ 147 (C-4), δ 69 (CH₂OH), δ 188 (CO), δ 205 [(CO)acyl], δ 50 (CH₃).

3a: Yield: 88%; Anal. found (calcd.) for C₁₀H₁₂ClINO₃Rh(%): C, 26.05 (26.14); H, 2.57 (2.61); N, 2.98 (3.04); selected IR data: 2070 [ν(CO) cm⁻¹], 1732 [ν(CO)_acyl cm⁻¹], ¹H NMR data (δ in ppm): δ 9.88 (H-1, d), 9.48–9.25 (H-2, m), δ 8.11–8.09 (H-3, m), δ 8.77–8.60 (H-4, m), δ 1.65 (CH₃, t), δ 2.59q (CH₂), 5.11s (CH₂OH), ¹³C NMR data (δ

in ppm): δ 163 (C-2), δ 124 (C-3), δ 135 (C-4), δ 69 (CH₂OH), δ 186 (CO), δ 207 [(CO)acyl], δ 58 (CH₂) δ 21 (CH₃).

3b: Yield: 86%; Anal. found (calcd.) for C₁₀H₁₂ClINO₃Rh(%): C, 26.06 (26.14); H, 2.59 (2.61); N, 3.02 (3.04); selected IR data: 2059 [ν(CO) cm⁻¹], 1731 [ν(CO)_acyl cm⁻¹], ¹H NMR data (δ in ppm): δ 9.61 (H-1, d), 9.42–8.72 (H-2, m), δ 7.67–7.20 (H-3, m), δ 8.50–8.45 (H-4, m), δ 1.87 (CH₃, t), δ 2.17q (CH₂), 4.64s (CH₂OH), ¹³C NMR data (δ in ppm): δ 155 (C-2), δ 134 (C-3), δ 137 (C-4), δ 68 (CH₂OH), δ 187 (CO), δ 206 [(CO)acyl], δ 60 (CH₂) δ 19 (CH₃).

3c: Yield: 87%; Anal. found (calcd.) for C₁₀H₁₂ClINO₃Rh(%): C, 26.15 (26.14); H, 2.49 (2.61); N, 2.98 (3.04); selected IR data: 2068 [ν(CO) cm⁻¹], 1726 [ν(CO)_acyl cm⁻¹], ¹H NMR data (δ in ppm): δ 9.12 (H-1, d), 7.86 (H-2, d), δ 2.1 (CH₃, t), δ 2.40q (CH₂), 4.68s (CH₂OH), ¹³C NMR data (δ in ppm): δ 156 (C-2), δ 124 (C-3), δ 146 (C-4), δ 68 (CH₂OH), δ 188 (CO), δ 206 [(CO)acyl], δ 61 (CH₂), δ 22 (CH₃).

2.4. Kinetic experiment

The kinetic experiments of **OA** reaction of complexes **1a**–**1c** with CH₃I were monitored using FTIR spectroscopy in a solution cell (CaF₂ windows, 1.0 mm path length). In order to obtained pseudo-first-order condition excess of CH₃I relative to metal complex was used. FTIR spectra (4.0 cm⁻¹ resolution) were scanned in the ν(CO) region (2200–1600 cm⁻¹) and saved at regular time interval using spectrum software. After completion of experiment, absorbance versus time data for the appropriate ν(CO) frequencies were extracted by substracting the solvent spectrum and analyzed off line using OriginPro 7.5 software. Kinetic measurements were made by following the decay of lower frequency ν(CO) band of the complexes **1** in the region 2018–2002 cm⁻¹. The pseudo-first-order rate constants were found from the gradient of the plot of ln(A_0/A_t) versus time, where A_0 is the initial absorbance and A_t is the absorbance at time t.

2.5. Carbonylation of methanol using [Rh(CO)₂ClL](**1**), L = 2-hydroxymethylpyridine (**a**), 3-hydroxymethylpyridine (**b**) and 4-hydroxymethylpyridine (**c**)

CH₃OH (0.099 mol, 4 cm³), CH₃I (0.016 mol, 1 cm³), H₂O (0.055 mol, 1 cm³) and complexes **1** (0.054 mmol) were taken into the reactor. The reactor was then purged with CO for about 5 min and then pressurized with CO gas (35 ± 5 bar). The carbonylation reactions were carried out at 130 ± 5 °C for 1 h. The products were collected and analyzed by G.C.

3. Results and discussion

3.1. Synthesis and characterization of the complexes [Rh(CO)₂ClL](**1**)

The reaction of [Rh(CO)₂Cl]₂ with two molar equivalents of pyridine alcohol ligands proceeds by symmetrical breakage of the dimer to afford the complexes of the type [Rh(CO)₂ClL](**1**) where L = 2-hydroxymethylpyridine (**a**), 3-hydroxymethylpyridine (**b**), 4-hydroxymethylpyridine (**c**) (Scheme 1). The observed elemental analyses data of the complexes agree well with their molecular composition. The IR spectra of the complexes **1a**–**c** exhibit two almost equal intense terminal ν(CO) bands in the region 2002–2090 cm⁻¹ indicating two carbonyl groups are mutually *cis* to one another [23,24]. It is interesting to note that the δ(OH) band of the ligands **a** and **b** occurred at 1596 cm⁻¹ and 1597 cm⁻¹, respectively whereas for **c**, it exhibited at 1609 cm⁻¹. Upon complexation with these ligands (**a**–**c**), the δ(OH) values do not show any characteristics shift towards lower frequency region suggesting that the −OH group remains uncoordinated, rather it shifted
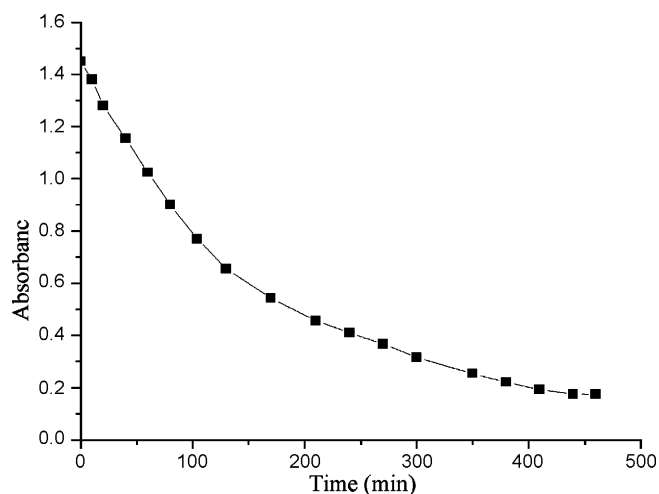
Scheme 1. Synthesis of rhodium carbonyl complexes containing pyridinealcohol ligands.

slightly towards high frequency region, which may be due to the breaking of intra/inter molecular hydrogen bonding [25,26]. The ^{1}H NMR spectra of the complexes **1a**–**c** exhibit a doublet resonance in the region δ 8.66–9.24 ppm for H-1 and multiplets in the region δ 7.38–8.97 ppm for H-2, H-3 and H-4 protons. The complexes exhibit characteristic resonance of substituted –CH$_2$ protons in the region δ 5.16–4.73 ppm. The ^{1}H NMR spectra of the free ligands **a**, **b** and **c** show a downfield shift when they involve in complex formation. These clearly indicate that the coordination to the metal center in the complexes **1** takes place through N-donor site. ^{13}C NMR spectra of the complexes **1a**–**c** show characteristic resonances of terminal carbonyl group in the range δ 183–185 ppm and pyridine carbon in the range δ 155–160 ppm, δ 124–133 ppm and δ 137–147 ppm for C-2, C-3 and C-4, respectively.

It is interesting to note that on storing the dicarbonyl complex **1a** in dichloromethane for about 10 days in presence of the ligand 2-hydroxymethylpyridine undergoes decarbonylation followed by oxidation resulting a chelated dimeric Rh(III) complex containing a very short symmetrical hydrogen bond [27].

3.2. Reactivity of the complexes 1 towards various electrophiles:

The complexes **1a**–**c** undergo **OA** reactions with electrophiles like CH$_3$I and C$_2$H$_5$I to yield the complexes [Rh(CO)(COCH$_3$)-ClIL](**2a**–**c**) and [Rh(CO)(COC$_2$H$_5$)ClIL](**3a**–**c**), respectively. Depending upon the stereochemical requirements the alkyl and halo group of the electrophiles may occupy *cis*- or *trans*- coordination sites to each other leading to formation of several possible isomers of the intermediates, which will undergo migratory insertion reaction to yield the final acyl products. The IR spectra of the products **2a**–**c** display ν(CO) absorption in the range 1727–1736 cm^{-1}, indicative of Rh(III)–acyl complex, resulting from facile migratory CO insertion in the complexes **1a**–**c** after oxidative addition of CH$_3$I (Scheme 2). Single intense terminal ν(CO) band in the range 2070–2082 cm^{-1} also indicates the formation of the oxidized products. Although the spectroscopic data do not provide definite structural characterization of the products **2a**–**c**, they are consis-

Fig. 1. Series of IR spectra {ν(CO) region} illustrating the reaction of **1b** (A) with MeI at 25 °C. The arrows indicate the behavior of each band as the reaction progresses. The bands of the products **2b** (C) are broad and shouldered due to presence of a mixture of isomers. The dotted lines express the spectra after completion of the reaction.

tent with a square pyramidal geometry with an apical acyl ligand as proposed in Scheme 2, as found for a number of other five-coordinated Rh(III)–acyl complexes of the type [RhL$_2$X$_2$(COCH$_3$)] [8,28–29]. Apart from the characteristic resonances of the ligands, the ^{1}H NMR spectra of complexes **2a**–**c** show a singlet in the region δ 2.96–3.38 ppm indicating the formation of –COCH$_3$ group. ^{13}C NMR spectra of the complexes **2a**–**c** show two carbonyl signals in the range δ 182–188 ppm for terminal carbonyl group and a poorly resolved slightly broad signal in the range δ 205–206 ppm for acetyl carbonyl group along with methyl carbon in the range δ 49–51 ppm and pyridine carbon in the range δ 155–160 ppm, δ 124–130 ppm and δ 136–145 ppm for C-2, C-3 and C-4, respectively. The broadness of the acetyl carbonyl signal may be due to the presence of isomers [30,31]. In a similar manner, **OA** of C$_2$H$_5$I with complexes **1a**–**c** also yield five-coordinated complexes [Rh(CO)(COC$_2$H$_5$)ClIL](**3a**–**c**). Similar to complexes **2a**–**c**, the IR spectra of the complexes show two different types of ν(CO) bands in the range 2059–2070 cm^{-1} and 1726–1732 cm^{-1} attributed to terminal and acyl ν(CO) values, respectively. The ^{1}H NMR spectra of the complexes **3a**–**c** show a triplet at around δ 1.65–2.15 ppm for methyl and a quartet in the region δ 2.17–2.59 ppm for methylene protons of the ethyl group. ^{13}C NMR spectra of the complexes **3a**–**c** show characteristic resonances of terminal and acetyl carbonyl group in the range δ 186–207 ppm and pyridine carbon in the range δ 155–165 ppm, δ 124–133 ppm and δ 137–147 ppm for C-2, C-3 and C-4, respectively.

Kinetic measurements for the **OA** reaction of the complexes **1a**–**c** with methyl iodide were carried out using IR spectroscopy to monitor the changes in the ν(CO). Fig. 1 shows a typical series of spectra, in which the bands due to **1b** decay and that due to **2b** grow until equilibrium is attained. The two terminal ν(CO) bands of

Scheme 2. OA reaction of RX with complexes **1**.

Fig. 2. Kinetic plot showing the decay of ν(CO) bands of **1b** during the reaction of **1b** with neat MeI at 25 °C.

the reactant **1b** at 2078 cm^{-1} and 2002 cm^{-1} were replaced by the terminal and acyl ν(CO) bands of the product **2b** at 2075 cm^{-1} and 1736 cm^{-1}, respectively. The spectrum of the product, **2b**, exhibits quite broad absorptions with shoulders, which are due to the presence of mixtures of isomers [30,31]. Absorbance versus time plots for the decay of lower intensity ν(CO) band (2078 cm^{-1}) of **1b** is shown in Fig. 2. A linear fit of pseudo-first-order was observed for the entire course of the reaction of CH$_3$I with the complexes **1** as is evidenced from the plot of $\ln(A_0/A_t)$ versus time, where A_0 and A_t are the absorbance at time $t = 0$ and t, respectively (Fig. 3). From the slope of the plot, the rate constants were calculated and found to be 4.6×10^{-5}, 7.83×10^{-5} and 6.83×10^{-5}, respectively for the complexes **1a**, **1b** and **1c**. The values of these rate constants clearly indicate that the rate of **OA** reaction of CH$_3$I with the complexes **1** follows an order **1b** > **1c** > **1a**. Nucleophilicity is a measure of electron density at the metal center, i.e. higher the electron density higher is its nucleophilicity. It also depends on the steric characteristics of ligands. From the order of appearance of CO stretching frequencies (**1c** > **1a** > **1b**) of the complexes **1**, it is observed that **1b** is highly nucleophilic and more prone towards the attack of electrophiles and expected to show high reactivity towards **OA** reaction.
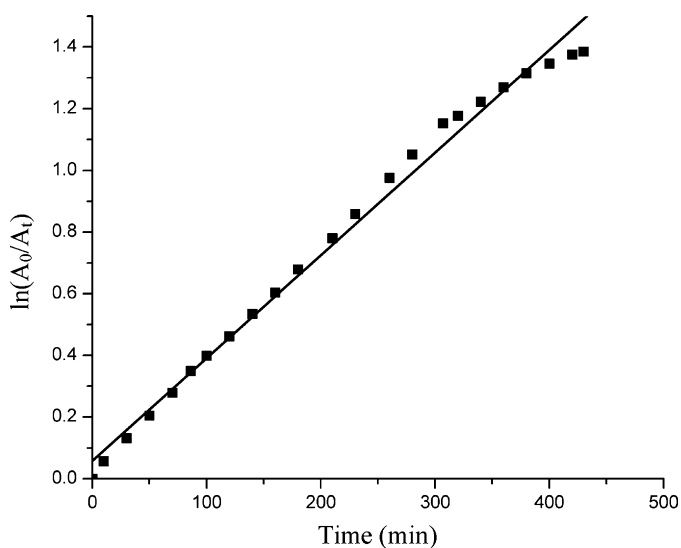

Fig. 3. Plot of $\ln(A_0/A_t)$ versus time for the **OA** reaction of the complex **1b** with neat MeI at 25 °C.

Table 1
Yield and TON of carbonylation reactions of methanol for 1 h reaction time

Catalysts	AcOH (%)	AcOMe (%)	Total conversion (%)	TON
[Rh(CO)$_2$Cl]$_2$	2.1	25.3	27.4	526
1a	3.5	27.7	31.2	600
1b	2.5	25.7	28.2	542
1c	4.7	29.1	33.8	649

TON = [amount of product (mol)]/[amount of catalyst (Rh mol)].

Due to the presence of electron withdrawing CH$_2$OH group at 3-position of pyridine ring, the ligand **b** donates more electron density to the metal center as compared to **a** and **c** resulting a lower value of CO stretching frequency for the complex **1b** and higher rate of **OA** reaction. Higher activity of **1c** over **1a** towards the **OA** of CH$_3$I may be due to the steric effect where the presence of hydroxymethyl substituent at 2-position of pyridine ring sterically restricts the path of incoming electrophiles resulting a slower reaction rate for the complex **1a**.

The kinetic study of **OA** reaction of CH$_3$I to [Rh(CO)$_2$I$_2$]$^-$ exhibiting two ν(CO) bands at 1988 cm^{-1} and 2045 cm^{-1}, generated *in situ* was also examined under similar experimental condition as described and found to proceed unexpectedly with a lower rate compared to the complexes **1** even showing ν(CO) bands in the higher region 2002–2090 cm^{-1}. This may be due to high electron density on the metal center establishing stronger M(d)–CO(π^*) back bonding which might considerably inhibit the CO insertion [32,33].

3.3. Catalytic activity of the complexes **1a–c**

The results of carbonylation of methanol to acetic acid and its ester in the presence of the complexes **1** and [Rh(CO)$_2$Cl]$_2$ as catalyst precursors are shown in Table 1. It appears that the highest turn over number (TON) 649 with corresponding conversion of about 34% is shown by the complex **1c** for 1 h reaction time. The complexes **1b** and **1a** exhibit moderate TON 542 and 600, respectively with corresponding conversion of about 28.2% and 31.2%. Under the same experimental condition, the well known catalyst precursor [Rh(CO)$_2$I$_2$]$^-$ generated *in situ* from [Rh(CO)$_2$Cl]$_2$ [4b], show the lowest TON 526 only with corresponding conversion of about 27.4%. The effect of different ligands on the efficiency of catalytic carbonylation reaction is clearly reflected and follows the order **1c** > **1a** > **1b** > [Rh(CO)$_2$I$_2$]$^-$. It is well known that higher the rate of **OA** reaction higher is the catalytic activity. Thus, the lower catalytic activity of [Rh(CO)$_2$I$_2$]$^-$ compared to the complexes **1** is substantiated by the observed trend in **OA** reaction. On the other hand, the trend in activities among the complexes **1a–c** towards catalytic carbonylation reaction cannot be explained by the observed trend of the rate of **OA** reaction. To explain this, one must consider the steric factors, hydrogen bonding, field effects etc. The highest catalytic activity shown by the complex **1c** may be due to the presence of hydroxymethyl substituent at sterically least hindered 4-position of the pyridine ring. The higher activity of the complex **1a** over **1b** may be due to the enhancement of nucleophilicity on the metal center by the neighboring group effect [34] where the 2-substituted hydroxymethyl substituent probably interacts with the metal centers by some non-conventional secondary interactions [18] and thus overcoming the steric hindrance.

Acknowledgements

References

[1] (a) M.J. Howard, M.D. Jones, M.S. Roberts, S.A. Taylor, Catal. Today 18 (1993) 325;
(b) K. Weissermel, H.J. Arpe, Industrial Organic Chemistry, third ed., Wiley-VCH, Weinheim, 1997.

[2] P.M. Maitlis, A. Haynes, G.J. Sunley, M.J. Howard, J. Chem. Soc., Dalton Trans. (1996) 2187.

[3] P.M. Maitlis, New Scientist 98 (1983) 208.

[4] (a) F.E. Paulik, J.F. Roth, Chem. Commun. (1968) 1578;
(b) D. Foster, J. Am. Chem. Soc. 98 (1976) 846.

[5] D. Foster, Adv. Organomet. Chem. 17 (1979) 255.

[6] D. Foster, T.C. Singleton, J. Mol. Catal 17 (1982) 299.

[7] C.M. Thomas, G.S. Fink, Coord. Chem. Rev. 243 (2003) 125.

[8] A. Haynes, B.E. Mann, G.E. Morris, P.M. Maitlis, J. Am. Chem. Soc. 115 (1993) 4093.

[9] L. Gonsalvi, H. Adams, G.J. Sunley, E. Ditzel, A. Haynes, J. Am. Chem. Soc. 124 (2002) 13597.

[10] E. Bouwman, M.A. Bolcar, E. Libby, J.C. Huffman, K. Folting, G. Christou, Inorg. Chem. 31 (1992) 5185.

[11] J.M. Berg, R.H. Kolm, J. Chem. Soc. Chem. Commun. (1993) 504.

[12] P.E. Hawkins, J.C. Dewan, K.B. Sharpless, Inorg. Chem. 25 (1986) 1501.

[13] L.A. Oro, M.P. Lamata, Trans. Met. Chem. 8 (1983) 48.

[14] N. Kumari, M. Sharma, P. Chutia, D.K. Dutta, J. Mol. Catal. A 222 (2004) 53.

[15] P. Das, M. Sharma, N. Kumari, D. Konwar, D.K. Dutta, Appl. Organomet. Chem. 16 (2002) 302.

[16] P. Das, P. Chutia, D.K. Dutta, Chem. Lett. (2002) 766.

[17] M. Sharma, N. Kumari, P. Das, P. Chutia, D.K. Dutta, J. Mol. Catal. A 188 (2002) 25.

[18] D.K. Dutta, J.D. Woollins, A.M.Z. Slawin, D. Konwar, P. Das, M. Sharma, P. Bhattacharyya, S.M. Aucott, J. Chem. Soc., Dalton Trans. (2003) 2674.

[19] D.K. Dutta, J.D. Woollins, A.M.Z. Slawin, D. Konwar, M. Sharma, P. Bhattacharyya, S.M. Aucott, J. Organometal. Chem. 691 (2006) 1129.

[20] N. Kumari, B.J. Sarmah, D.K. Dutta, J. Mol. Catal. A 266 (2006) 260.

[21] P. Chutia, B.J. Sarmah, D.K. Dutta, Appl. Organomet. Chem. 20 (2006) 512.

[22] J.A. Mccleverty, G. Wilkinson, Inorg. Synth. 8 (1966) 221.

[23] L.M. Vallarino, S.W. Sheargold, Inorg. Chim. Acta 36 (1979) 243.

[24] D.K. Dutta, M.M. Singh, Trans. Met. Chem. 19 (1994) 290.

[25] D. Dolphine, A. Wick, Tabulation of IR spectral data, Wiley & Sons, New York, 1977, p. 304.

[26] K. Nakamoto, Infrared Spectra of Inorganic and Coordination Compounds, second ed., Wiley, New York, 1970, p. 232.

[27] B.J. Sarmah, D.K. Dutta, unpublished work.

[28] H. Adams, N.A. Bailey, B.E. Mann, C.P. Manuel, Inorg. Chim. Acta 198–200 (1979) 111.

[29] K.G. Moloy, J.L. Peterson, Organometallics 14 (1995) 2931.

[30] A. Hynes, B.E. Mann, G.E. Morris, P.E. Maitlis, J. Am. Chem. Soc. 115 (1993) 4093.

[31] H. Adams, N.A. Bailey, B.E. Mann, C.P. Manuel, C.M. Spencer, A.G. Kent, J. Chem. Soc., Dalton Trans. (1988) 489.

[32] L. Gonsalvi, H. Adams, G.J. Sunley, E. Ditzel, A. Haynes, J. Am. Chem. Soc. 121 (1999) 11233.

[33] P. Margl, T. Ziegler, P.E. Blochl, J. Am. Chem. Soc. 118 (1996) 5412.

[34] J.C. Jeffrey, T.B. Rauchfuss, Inorg. Chem. 18 (10) (1979) 2658.